Investigation of field-induced ferromagnetism in Pd–Ni–Fe–P metallic glass by x-ray magnetic circular dichroism

D. H. Yu,[1,a)] J. Duriavig,[1] N. Loh,[1,2] R. Woodward,[2] H. J. Lin,[3] F. H. Chang,[3] S. H. Kilcoyne,[4] A. Stampfl,[1,5] and R. A. Robinson[1]
[1]*Bragg Institute, Australian Nuclear Science and Technology Organisation, Lucas Height, New South Wales 2234, Australia*
[2]*School of Physics, University of Western Australia, 35 Stirling Highway, Crawley, Western Australia 6009, Australia*
[3]*National Synchrotron Radiation Research Center, 101 Hsin-Ann Road, Hsinchu Science Park, Hsinchu 30076, Taiwan*
[4]*Institute of Materials Research, University of Salford, Salford M5 4WT, United Kingdom*
[5]*School of Chemistry, The University of Sydney, New South Wales 2006, Australia*

(Received 3 October 2008; accepted 20 December 2008; published online 13 January 2009)

We have applied x-ray magnetic circular dichroism to investigate the field-induced ferromagnetism in $Pd_{40}Ni_{22.5}Fe_{17.5}P_{20}$ alloy. The experiment revealed that both Ni and Fe were in a divalent state and that the magnetic properties of the material were determined by the localized 3*d* electrons of the transition metals. No clear evidence of Ruderman–Kittel–Kasuya–Yosida-type interaction among magnetic clusters was observed. It is believed that the detailed balance of fundamental spin-orbit and exchange interactions as a function of temperature and applied magnetic field determine the different magnetic properties of the alloy.
[DOI: 10.1063/1.3070528]

The metallic glass of the $Pd_{40}(Ni_{1-x}Fe_x)_{40}P_{20}$ alloy possesses interesting magnetic properties, including paramagnetic, superparamagnetic, and spin glass phases as a function of temperature and applied magnetic field. An interesting observation by Shen *et al.*[1] was the existence of a *field-induced ferromagnetic phase* in amorphous $Pd_{40}Ni_{22.5}Fe_{17.5}P_{20}$. The formation mechanism of the field-induced ferromagnetic phase is not yet well understood. Hsiao *et al.*[2] suggested that interaction among magnetic/chemical inhomogeneities through Ruderman–Kittel–Kasuya–Yosida (RKKY) coupling across the Pd-rich matrix may contribute to the complex magnetic properties of the alloy. Different cluster sizes of 30–40, 200, and 20 Å have been reported.[2,3]

For $Pd_{40}Ni_{40}P_{20}$ the effective moment of nickel is $0.109\mu_B$/atom, which is double that of the $Ni_{80.2}P_{19.8}$ alloy as a result of the induced polarization of neighboring Pd atoms.[1] For $Pd_{40}Ni_{40-x}Fe_xP_{20}$ ($x=5-17.5$) Shen *et al.*[1] calculated an effective moment of $5.6-6.4\mu_B$/Fe atom, assuming that the magnetic moment of the Ni was 0. They suggested that the enhanced Fe moment was also due to a strong spin polarization of Pd-rich matrix. Although a classical interpretation of RKKY interaction, based on the system with unperturbed paramagnetic matrix, may not be applicable to the system containing Pd whose paramagnetic ground state may be strongly modified by the magnetic impurities and thus carrying induced magnetic moment,[4] a similar type of coupling may be responsible for the formation of the field-induced ferromagnetism of the $Pd_{40}Ni_{22.5}Fe_{17.5}P_{20}$. We report on studies of individual magnetic moments of Fe, Ni, and Pd for the $Pd_{40}Ni_{22.5}Fe_{17.5}P_{20}$ alloy by x-ray magnetic circular dichroism (XMCD), aiming to identify the origin of the field-induced ferromagnetism.

The $Pd_{40}Ni_{22.5}Fe_{17.5}P_{20}$ ribbon, prepared by rf melt spinning,[5] has been characterized using a superconducting quantum interface device (SQUID) magnetometer, and the same phase behavior as reported by Shen *et al.*[1] has been confirmed. The XMCD experiment was conducted at the Dragon beam line at the National Synchrotron Radiation Research Centre in Taiwan.[6] The sample temperature was 17 K and the applied magnetic field was 1 T, corresponding to the induced ferromagnetic phase of the alloy. The field was along the length direction (*y*-axis) in the surface plan of the sample. The propagation direction of the incident circular polarized light (about 80% polarization) was 30° with respect to the surface of the sample. The total electron yield mode was used for the measurements of x-ray absorption spectra (XAS). The XMCD spectra correspond to the difference of the spin-resolved XAS with two opposite magnetic field directions after proper background subtraction.[7] The magnetic moments were derived using the XMCD sum rules.[8] Oxidation of the top monolayers of the sample could not be excluded. However the measurement should mainly probe the bulk properties of the alloy as the probe depth of the total electron yield is of the order of 10 nm.

Figures 1 and 2 present the Ni and Fe 2*p* isotropic XAS and XMCD, respectively. Multiple structures have been observed as marked by capital letters from A to F in the figures. For Ni, two distinct peaks appear at both L_2 and L_3 edges, while three peaks can be identified from the corresponding Fe 2*p* XAS.

The double peak structures of the Ni 2*p* XAS have been predicated theoretically[9] and observed experimentally in several compounds, for example, Ni dihalides and NiO,[10] Ni oxalate,[11] and $NiFe_2O_4$ (trevorite).[12] The 17 eV splitting between peaks A and C corresponds to the L_2 and L_3 separations due to the large spin-orbit interaction of the core level. The splitting between peaks A and B is a measure of the 2*p* hole and 3*d* electron exchange interaction. The mea-

a)Electronic mail: dyu@ansto.gov.au.

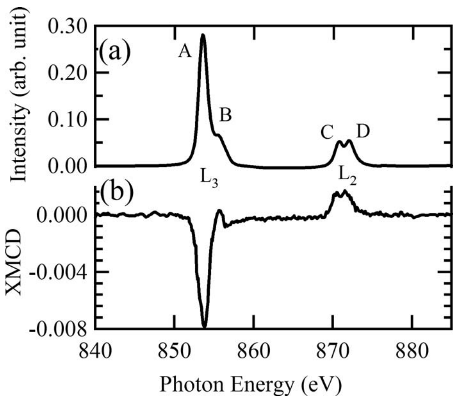

FIG. 1. Ni $2p$ (a) XAS and (b) XMCD at $T=17$ K and $B=1$ T.

sured splitting in the $Pd_{40}Ni_{22.5}Fe_{17.5}P_{20}$ compound is 1.78 ± 0.06 eV, which is less than the values of 2 and 1.9 eV observed for trevorite and NiO, respectively.[12] Similar to the case for trevorite,[12] peak A corresponds to the transition under spin conservation, while peak B is from a spin-flip transition, due to the strong $2p$ spin-orbit interaction. The spin-flip process is further reflected by the opposite dichroism of peaks A and B in the XMCD spectrum [Fig. 1(b)]. Similar processes are responsible for the double peaks at the L_2 edge, but with less pronounced spin-flip effects due to the nonpure spin states involved in the transitions.[13]

The measured Ni $2p$ XAS and XMCD spectra are consistent with the existing atomic multiplet calculations in a crystal field with local octahedral symmetry for free Ni^{2+} ion with initial $3d^8$ and final $\underline{2p}3d^9$ configurations.[9,12] Coulomb, spin-orbit, exchange interactions, and interatomic screening and states mixing effects were included in the calculations for both initial and final states. The calculated spectra with crystal field strengths larger than 1 eV approached the experimental observations for $Pd_{40}Ni_{22.5}Fe_{17.5}P_{20}$. For the isotropic branching ratios $B(i)$, defined as the integrated intensity of the L_3 edge normalized to the integrated intensity of the whole XAS,[9] our measured value is 0.779 ± 0.009, which is in good agreement with the calculated value of $B(i)=0.75$ corresponding to the high-spin ground state with 1 eV crystal field strength.[9]

The orbital-to-spin magnetic moments ratio (L/S) for Ni from $Pd_{40}Ni_{22.5}Fe_{17.5}P_{20}$ is 0.33 ± 0.06, obtained using XMCD sum rules. The value agrees well with the results of 0.27 ± 0.07 and 0.34 ± 0.11 from trevorite.[12] This indicates that the localized $3d$ electrons determine the Ni magnetic properties in both compounds, which are well described by the atomic calculations.

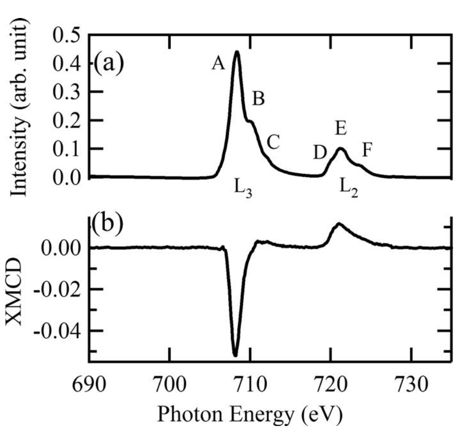

FIG. 2. Fe $2p$ (a) XAS and (b) XMCD at $T=17$ K and $B=1$ T.

TABLE I. Magnetic moments for Fe and Ni; Pure element values are quoted from Refs. 8 and 13.

Moment/atom (μ_B)	Present work	Pure element[a]	Present work	Pure element[b]
Element	Fe	Fe	Ni	Ni
Orbital (L)	0.0511	0.086	0.0579	0.05
Spin (S)	0.5240	1.98	0.1754	0.52
L/S	0.0975	0.043	0.3301	0.096
Total	0.5751	2.066	0.2333	0.57

[a]Reference 8.
[b]Reference 13.

For Fe, a similar atomic calculation has been reported based on the transition of $3d^6 \rightarrow \underline{2p}3d^7$ of Fe^{2+}.[9] The XAS and XMCD spectra agree qualitatively with the present measurement. Our experimental isotropic branching ratio of 0.788 ± 0.003 agrees very well with the calculated values of $B(i)=0.78$ for the high-spin ground state. Theory[9] also predicted the triple peak structure at the L_3 edge. This provides evidence that the localized $3d$ electrons also dominate the magnetic properties of the Fe in the $Pd_{40}Ni_{22.5}Fe_{17.5}P_{20}$ compound.

The orbital and spin magnetic moments for Fe and Ni are listed in Table I, with 20% uncertainties mainly from the errors in the light polarization and background subtractions. For comparison the values for pure Fe and Ni measured with XMCD under saturation conditions by Chen *et al.*[8,13] are also listed in the Table I.

For both Fe and Ni, finite magnetic moments have been derived. At $T=17$ K and $B=1$ T, the total magnetic moment of 11.9 emu/g derived from XMCD agrees well with our measured value of 13.7 emu/g using SQUID magnetometry. As compared to the pure elements, much smaller total magnetic moments for Fe and Ni were obtained. This may partially be due to the fact that the material is far from reaching saturation with the 1 T applied field here. However, the L/S values of Fe and Ni from $Pd_{40}Ni_{22.5}Fe_{17.5}P_{20}$ alloy are much larger than those from the pure elements. This indicates that the enhancement of orbital moments of Fe and Ni contributes to the total magnetic moment. The total Ni magnetic moment is approximately 40% of the Fe moment, which is substantial.

The comparison of the XMCD signal for Fe, Ni, and Pd is presented in Fig. 3. Iron is the dominant carrier of the magnetic moment as evidenced by its about ten times larger L_3 edge dichroism than that from the Ni L_3 edge. The XMCD signal at the Pd M_3 edge is about ten times smaller than that of Ni at L_3 edge. Since the sign of the Pd XMCD was not observed to change when the polarization state of light was changed, we conclude that there was no measurable XMCD from Pd M_3 edge within the limits of the current experiment. Due to the excitation range of the instrument, the XMCD at the Pd L edge has not yet been measured. The Pd L edge may show discernible XMCD signal.[14] The failure to observe dichroism from the Pd M_3 edge does not totally exclude the RKKY interaction through the Pd matrix. Further studies are planned to measure XMCD at the Pd L edge to investigate the role of RKKY interaction in the formation of field-

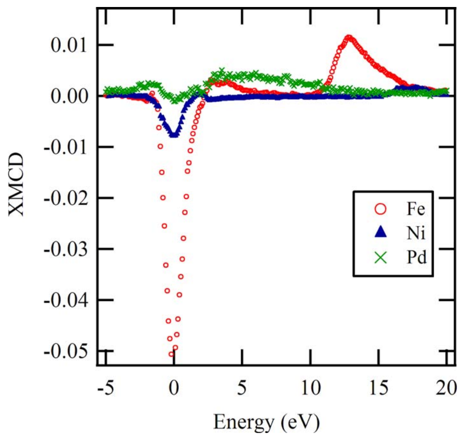

FIG. 3. (Color online) XMCD for Fe (circle), Ni (filled triangle), and Pd (cross) at $T=17$ K and $B=1$ T. Note that the energy axis is shifted with respect to the first peak positions for the three elements.

induced ferromagnetism. Nevertheless our observations do show that the localized 3d electrons of Fe and Ni determine the overall magnetic properties of the alloy. The strong temperature and magnetic field dependence of the magnetic properties of the alloy may be originated from spin-orbit and exchange interactions which are of the order of kT.

In summary, individual magnetic moments from Ni and Fe in the $Pd_{40}Ni_{22.5}Fe_{17.5}P_{20}$ metallic glass have been determined by XMCD in the field-induced ferromagnetic phase. While Fe is the dominant carrier of magnetic moment, Ni contributes significantly to the total magnetic moment of the material. The enhancement of orbital magnetic moments of Ni and Fe makes a large contribution to the overall magnetic moments of the material. The experiment shows that the localized 3d electrons of Ni and Fe may determine the magnetic properties of the alloy, through the detailed balance of fundamental spin-orbit and exchange interactions as a function of temperature and applied magnetic field.

The support from the Australian Synchrotron Research Program is gratefully acknowledged. We thank Dr. Frank Klose for useful discussions and comments on the draft.

[1]T. D. Shen, R. B. Schwarz, and J. D. Thompson, J. Appl. Phys. **85**, 4110 (1999).
[2]A. C. Hsiao, L. H. Lewis, K. Kang, and A. R. Moodenbaugh, J. Appl. Phys. **99**, 08F117 (2006).
[3]D. H. Yu, M. R. Fitzsimmons, E. P. Gilbert, R. C. Woodward, S. H. Kilcoyne, and R. A. Robinson, Physica B **397**, 30 (2007).
[4]O. Rader, E. Vescovo, J. Redinger, S. Blugel, C. Carbone, W. Eberhardt, and W. Gudat, Phys. Rev. Lett. **72**, 2247 (1994).
[5]S. H. Kilcoyne, P. M. Bentley, and D. Greig, J. Magn. Magn. Mater. **272**, 1383 (2004).
[6]C. T. Chen, Nucl. Instrum. Methods Phys. Res. A **256**, 595 (1987); C. T. Chen and F. Sette, Rev. Sci. Instrum. **60**, 1616 (1989).
[7]H. J. Elmers, G. H. Fecher, D. Valdaitsev, S. A. Nepijko, A. Gloskovskii, G. Jakob, G. Schonhense, S. Wurmehl, T. Block, C. Felser, P. C. Hsu, and W. L. Tsai, Phys. Rev. B **67**, 104412 (2003).
[8]C. T. Chen, Y. U. Idzerda, H.-J. Lin, N. V. Smith, G. Meigs, E. Chaban, G. H. Ho, E. Pellegrin, and F. Sette, Phys. Rev. Lett. **75**, 152 (1995).
[9]G. van der Laan and B. T. Thole, Phys. Rev. B **43**, 13401 (1991).
[10]G. van der Laan, J. Zaanen, G. A. Sawatzky, R. Karnatak, and J.-M. Esteva, Phys. Rev. B **33**, 4253 (1986).
[11]G. van der Laan, B. T. Thole, and G. A. Sawatzky, Phys. Rev. B **37**, 6587 (1988).
[12]G. van der Laan, C. M. B. Henderson, R. A. D. Pattrick, S. S. Dhesi, P. F. Schofield, E. Dudzik, and D. J. Vaughan, Phys. Rev. B **59**, 4314 (1999).
[13]C. T. Chen, N. V. Smith, and F. Sette, Phys. Rev. B **43**, 6785 (1991).
[14]M. A. Tomaz, T. Lin, G. R. Harp, E. Hallin, T. K. Sham, and W. L. O'Brien, J. Vac. Sci. Technol. A **16**, 1359 (1998).